

1 **Increases in aridity lead to drastic shifts in the assembly of dryland complex microbial networks**

2

3 Manuel Delgado-Baquerizo^{1,2*}, Guilhem Doullcier^{3,4}, David J. Eldridge⁵, Daniel B. Stouffer⁴, Fernando
4 T. Maestre⁶, Juntao Wang², Jeff R. Powell², Thomas C. Jeffries², Brajesh K. Singh^{2,7}.

5

6 1. Cooperative Institute for Research in Environmental Sciences, University of Colorado, Boulder, CO
7 80309.

8 2. Hawkesbury Institute for the Environment, Western Sydney University, Penrith, 2751, New South
9 Wales, Australia.

10 3. Institut de Biologie de l'École Normale Supérieure, École Normale Supérieure, PSL Research
11 University, Paris, France.

12 4. Centre for Integrative Ecology, School of Biological Sciences, University of Canterbury, Private
13 Bag 4800, Christchurch 8140, New Zealand

14 5. Centre for Ecosystem Science, School of Biological, Earth and Environmental Sciences, University
15 of New South Wales, Sydney, New South Wales, 2052, Australia.

16 6. Departamento de Biología, Geología, Física y Química Inorgánica, Escuela Superior de Ciencias
17 Experimentales y Tecnología, Universidad Rey Juan Carlos, c/ Tulipán s/n, 28933 Móstoles, Spain.

18 7. Global Centre for Land-Based Innovation, Western Sydney University, Penrith South DC, NSW
19 2751, Australia.

20 ***Author for correspondence:**

21 Manuel Delgado-Baquerizo. Cooperative Institute for Research in Environmental Sciences, University
22 of Colorado, Boulder, CO 80309. E-mail: M.DelgadoBaquerizo@gmail.com

23

24

25

26

27

28

29

This is the author manuscript accepted for publication and has undergone full peer review but has not been through the copyediting, typesetting, pagination and proofreading process, which may lead to differences between this version and the Version of Record. Please cite this article as doi: [10.1002/ldr.3453](https://doi.org/10.1002/ldr.3453)

30 **Abstract**

31 We have little information on how and why soil microbial community assembly will respond to
32 predicted increases in aridity by the end of this century. Here, we used correlation networks and
33 structural equation modeling to assess the changes in the abundance of the ecological clusters including
34 potential winner and loser microbial taxa associated with predicted increases in aridity. To do this, we
35 conducted a field survey in an environmental gradient from eastern Australia, and obtained information
36 on bacterial and fungal community composition for 120 soil samples, and multiple abiotic and biotic
37 factors. Overall our structural equation model explained 83% of the variance in the two mesic modules.
38 Increases in aridity led to marked shifts in the abundance of the two major microbial modules found in
39 our network, which accounted for >99% of all phylotypes. In particular, the relative abundance of one
40 of these modules, the Mesic-Module-#1, which was positively related to multiple soil properties and
41 plant productivity, declined strongly with aridity. Conversely, the relative abundance of a second
42 dominant module (Xeric-Module-#2) was positively correlated with increases in aridity. Our study
43 provides evidence that network analysis is a useful tool to identify microbial taxa that are either
44 winners or losers under increasing aridity and therefore potentially under changing climates. Our work
45 further suggests that climate change, and associated land degradation, could potentially lead to
46 extensive microbial phylotypes exchange and local extinctions, as demonstrated by the reductions of up
47 to 97% in the relative abundance of microbial taxa within Mesic-Module-#1.

48

49 **Key words.** Global Change Ecology; Ecological networks; Fungi; Bacteria; Soil functions; Climate
50 change; Plant-soil interactions.

51

52

53

54

55 **Introduction**

56 Climate change is leading to a drier and hotter world and resulting in major soil degradation processes
57 (Huang et al. 2016). Drylands already occupy over 45% of Earth's landmass, with their cover expected
58 to further increase by up to 23% by the end of this century (Huang et al. 2016). In drylands, soil
59 bacteria and fungi are the most diverse and abundant organisms, and play critical roles in maintaining
60 the rates and stability of multiple ecosystem functions, including litter decomposition, primary
61 production, soil fertility and gas exchange (Delgado-Baquerizo et al. 2017). However, the diversity and
62 abundance of fungi and bacteria are also highly vulnerable to climate change (Maestre et al. 2015).
63 Microbial communities exhibit complex connections involving a large number of inter- and intra-
64 dependent interactions, making it very difficult to predict how entire microbial communities are likely
65 to respond to global environmental change (Rillig et al. 2015; Shi et al. 2016). Some taxa can
66 potentially benefit from increases in aridity (winners), while other taxa will be hindered as aridity
67 increases (losers; *sensu* Eldridge et al. 2018a). Identifying potential winner and loser taxa in response to
68 increases in aridity could have potential future implications for the management of microbial
69 communities under global change scenarios. Network analysis has recently been proposed as a
70 promising approach to describe this complexity and to obtain deeper insights into the organization of
71 microbial associations in terrestrial ecosystems (Shi et al. 2016). The structure of ecological networks,
72 which integrates biodiversity, community composition, and ecosystem functioning (Tylianakis et al.
73 2008), is also regarded as a key attribute of biotic communities. Thus, taking a whole-network approach
74 has the potential to advance our knowledge of microbial community and ecosystem responses to global
75 change drivers (e.g., climate change) at both local and global scales (Barberán et al. 2012; Rillig et al.
76 2015; Neilson et al. 2017).

77 Recent studies have demonstrated that soil microbial taxa strongly associate with each other,
78 and lead to the formation of well-defined modules (nodes of fungi or bacteria, also called ecological
79 clusters) of taxa, providing evidence for tightly synchronized responses among bacteria and fungi (Shi
80 et al. 2016). Moreover, previous studies have provided evidence that specific taxa of fungi and bacteria
81 can share certain environmental preferences (Barberán et al. 2012; Rillig et al. 2015). Thus, they share
82 similar predictors, such as location (distance from the equator), climate (e.g. aridity and temperature)
83 and soil properties (e.g. pH and nutrients; Ramirez et al. 2014, Tedersoo et al. 2014; Maestre et al.
84 2015). This suggests that particular bacterial and fungal taxa may strongly co-occur in soils across

85 environmental gradients. Unlike traditional analyses, more focus on the microbial diversity and
86 community composition and, the identification of highly connected modular structures representing
87 important ecological units (Shi et al. 2016; Delgado-Baquerizo et al. 2018a) provide a unique
88 opportunity to integrate highly multi-dimensional data (i.e., such as those from microbial communities),
89 allowing more robust statistical inferences on the major predictors of entire microbial communities
90 (Duran-Pinedo and others, 2011; Shi et al. 2016).

91 Microbial modules have recently been reported to represent highly dynamic ecological
92 structures that respond to changing environmental conditions. For example, Nuccio et al. (2016) and
93 Shi et al. (2016) showed that the modularity of microbial networks from plant rhizospheres responds to
94 biological activity during a growing season. Much less is known, however, about how changes in
95 climate, such as predicted increases in aridity (Huang et al. 2016), affect the network of associations
96 among bacterial and fungal taxa within drylands (Neilson et al. 2017). Increasing aridity may alter the
97 relative abundance of modules both directly (i.e. via reductions in water availability; Maestre et al.
98 2015), and indirectly (via changes in soil properties and plant attributes; Delgado-Baquerizo et al.
99 2016). For example, increases in soil pH associated with increasing aridity can influence the diversity
100 and community composition of soil bacteria and fungi (Rousk et al. 2010; Maestre et al. 2015), and as
101 such could affect soil microbial networks.

102 Here we applied network analyses and statistical modeling to data from a regional survey
103 (>1000 km) spanning a wide range of aridity conditions and three within-plot vegetation types (Fig. 1)
104 to test the hypothesis that increases in aridity such as those forecasted under climate change will result
105 in substantial shifts in the relative abundance of microbial modules, leading to a new network of
106 microbial associations in soils in ecosystems from eastern Australia. More importantly, we aim to
107 identify a list of winner and loser taxa in response to potential increases in aridity in eastern Australia
108 (Huang et al. 2016).

110 **Material and Methods**

111 *Study area*

112 We conducted this study at twenty locations from eastern Australia (Fig. 1A). Locations for this study
113 were chosen to include a wide range of aridity levels including arid, semiarid and dry-subhumid
114 ecosystems. The total annual precipitation and mean temperature in this region ranged from 280 mm to

115 1167 mm and from 12.8° C to 17.5°C, respectively. The locations included in this study showed a wide
116 variety of vegetation types (e.g., grasslands, shrublands, savannas, dry seasonal forests and open
117 woodlands dominated by trees). Perennial plant cover in these plots ranged between 18 to 98%.

118 *Soil sampling*

119 Soils were sampled in in the Australian summer (March 2014). Within each site we selected a 30 m x
120 30 m plot which represented the dominant vegetation within each location. Plant cover and richness
121 were measured within each plot as explained in Maestre et al. (2015). We collected three composite soil
122 samples (three 0-5 cm depth soil cores) from beneath the vegetation (N-fixing shrubs, grasses, and
123 trees) and in open areas between plant patches at each site. The same plant taxa were present across the
124 complete gradient of aridity: *Eucalyptus* spp., *Acacia* spp. and the C3 native grass *Rhytidosperma* spp.
125 A total of 120 soil samples (20 sites x 6 within-plot composite samples) were collected in this study.
126 Note that we used a stratified sampling design to maximize within-plot spatial variability, which is
127 critical for building co-occurrence networks based on correlations. Our sampling design also allows the
128 comparison of information collected across plots, which otherwise (i.e., random sampling design)
129 might have differed in terms of spatial variability. Soil samples were sieved (2 mm mesh). Then,
130 portion of soil was immediately frozen at -20 °C for molecular analyses, while the rest of the soil was
131 air-dried, and stored for one month, before physicochemical analyses.

132 *Soil properties.*

133 Soil total organic C content was determined using the method described in Maestre et al. (2015). Soil
134 total N was measured with a CNH analyzer (Leco CHN628 Series, LECO Corporation, St Joseph, MI,
135 USA). Soil pH was measured in all the soil samples (1: 2.5 soil/water suspension). Total P was
136 measured after digestion with sulphuric acid using a SKALAR San++ Analyzer (Skalar, Breda, The
137 Netherlands). Soil total P was positively and significantly correlated with microbial biomass P ($\rho =$
138 0.18 ; $P = 0.049$), Olsen inorganic P ($\rho = 0.45$; $P < 0.001$) and plant leaf P content ($\rho = 0.23$; $P = 0.027$),
139 and, therefore, is a good surrogate of P availability. Total P ranged from 17 to 600 mg P kg⁻¹ soil. Soil
140 total organic C ranges from 0.7 to 12%. Soil pH ranged from 4.8 to 9.1.

141 *Surrogates of ecosystem functioning.*

142 We measured: (1) the activities of three soil enzymes using the method explained in Bell et al. (2013):
143 α -glucosidase (starch degradation), N-acetyl- β -Glucosaminidase (chitin degradation) and phosphatase
144 (organic phosphorus mineralization), (2) the availability of dissolved organic carbon and inorganic N

145 from K₂SO₄ extracts measured as described in Delgado-Baquerizo et al. (2016), and (3) aboveground
146 net primary productivity (ANPP) for the whole of 2014 and for March 2014, the month in which soil
147 sampling was conducted, using NDVI obtained from satellite data as described in Delgado-Baquerizo
148 et al. (2018a).

149 *Environmental variables*

150 For each site we calculated the aridity level [1 – Aridity Index (AI), where AI is precipitation/potential
151 evapotranspiration] using AI data from the database in Maestre et al. (2015). We used aridity rather
152 than mean annual precipitation because aridity is a more appropriate variable which includes both mean
153 annual precipitation and potential evapotranspiration. Furthermore, this variable provides an integrative
154 measure of the long-term water availability at each site. Finally, we identified the soil type in each plot
155 using available data from the ISRIC (global gridded soil information) Soil Grids ([https://soilgrids.org/
156 #/?layer=geonode:taxnwr_b_250m](https://soilgrids.org/#/?layer=geonode:taxnwr_b_250m)), which provide global information on soil classification (USDA
157 classification) at a 250m resolution.

158 *Molecular analyses*

159 Soil DNA was extracted from 0.25 g of soil samples (defrosted) using the Powersoil® DNA Isolation
160 Kit (Mo Bio Laboratories, Carlsbad, CA, USA). We quantified the total abundance bacteria and fungi
161 in all soil samples using 96-well plates on a CFX96 Touch™ Real-Time PCR Detection System (Foster
162 city, California, USA; qPCR). We used the primer sets: Eub 338-Eub 518 and ITS 1-5.8S described in
163 Maestre et al. (2015) for qPCR analyses. We then employed amplicon sequencing using the Illumina
164 MiSeq platform to characterize the community composition of bacteria and fungi in our samples . We
165 used the 341F/805R (bacteria) and FITS7/ITS4 (fungi) primer sets (Maestre et al. 2015) for these
166 analyses. Bioinformatic processing was performed using a combination of QIIME (Caporaso et al.
167 2010), USEARCH (Edgar 2010) and UCLUST (Edgar 2010). Operational Taxonomic Units (OTUs;
168 phylotypes hereafter) were defined as clusters of 97% sequence similarity using UCLUST (Edgar
169 2010). Taxonomy was assigned using against the Greengenes database version 13_850 for 16S rDNA
170 OTUs (DeSantis et al. 2006). For fungal ITS sequences, taxonomy was assigned using the UNITE
171 database V6.9.7 ($E < 10^{-5}$) (Koljalg et al. 2013). We filtered the OTU abundance tables for both primer
172 sets to remove singletons. We then rarefied to an even number of sequences per samples to ensure an
173 equal sampling depth (11789 and 16222 for 16S rDNA and ITS respectively).

174 *Network analyses*

175 We first built a single correlation network between the phylotypes within the abundance table using the
176 following protocol aiming to identify modules of strongly co-occurring microbial taxa. Prior to these
177 analyses, we filtered out the rarest phylotypes by removing those with less than five reads in at least
178 one sample across all samples. This resulted in a network with 25084 phylotypes as nodes (10570
179 bacterial and 14514 fungal phylotypes, respectively). We then calculated all pairwise Spearman
180 correlation coefficients among these microbial taxa and kept all positive correlations. This non-
181 parametric method measures the strength and direction of association between two ranked variables.
182 We focused exclusively on positive correlations because they provide useful information on the co-
183 occurrence of particular microbial taxa that may respond in a similar manner to particular
184 environmental conditions such as increases in aridity (Barberan et al. 2012). This approach ultimately
185 allowed us to address our research question on the role aridity in regulating the relative abundance of
186 the main microbial modules composed by bacterial and fungal taxa strongly co-occurring with each
187 other. This led to a network with 62,388,880 links, which corresponds to just 19.8% of all possible links
188 (falling within the expected range from previous ecological networks; Stouffer and Bascompte 2011).
189 In all instances, we weighted these links by their corresponding correlation coefficient. We then used
190 the Markov Cluster Algorithm software (van Dongen 2000) to extract modules from the network. This
191 algorithm is explicitly designed to efficiently handle large networks. Here, a single parameter controls
192 the quality of the clustering output. Rather than using the default options, we adjusted the inflation
193 parameter to maximize the modularity of the resulting partition, which is a quantitative measure of the
194 quality of a given partitioning of nodes in a network (Newman 2004). We used an inflation parameter I
195 $= 2.8$, which lead to a maximum modularity $M=0.124951$ based on the assignment of phylotypes to
196 four separate modules. We then calculated the relative abundance of these modules by summing the
197 relative abundances (%) of all phylotypes within each module. Finally, we computed the relative
198 abundance of each module in each site as the average relative abundance in the site's samples weighted
199 by the coverage of the corresponding microhabitats (vegetation and open areas). Using this approach,
200 we focus on the relative abundance of modules, rather than on individual taxa.

201 After obtaining this co-occurrence network and detecting the modules within this network, we
202 proceeded to cross-validate our network using an independent approach. To do this we first calculated
203 all pairwise SparCC correlations between bacterial and fungal nodes using the Fastspar algorithm
204 (Friedman & Alm, 2017), with 100 bootstraps and 100 permutations to control false discovery rate. For

205 these analyses we used a more conservative approach than that described above and used a minimum
206 correlation coefficient of 0.4 and $P < 0.05$. Finally, we used the algorithm introduced by Vincent et al.
207 (2008) to extract modules from the network. The relative abundance of these modules was calculated as
208 the average of the standardized relative abundances (z-score) of all phylotypes within each module.

209 *Statistical analyses*

210 We evaluated the effect of aridity on the relative abundance of different microbial clusters (or modules)
211 using linear regressions. To account for the spatial influence of the data (latitude and longitude), we
212 used spatial autoregressive analyses. We used structural equation modeling (SEM, Grace 2006) to
213 evaluate the direct and indirect effects of aridity and other important predictors of soil microbial
214 communities like the distance from the equator, soil type and properties (total C, P and pH), within-plot
215 vegetation type (trees, shrubs, grasses), plant cover and richness and microbial attributes (fungal and
216 bacterial abundance and ratio), on the relative abundance of detected microbial modules. Thus, we used
217 SEM to further clarify the effects of aridity on the relative abundance of each microbial module
218 after taking into account statistically various environmental factors simultaneously (see our *a priori*
219 model in Fig. S1). Changes in soil properties, plant attributes and microbial abundance due to
220 increasing aridity could potentially affect the role that the environment plays in microbial associations,
221 and this will likely influence the assembly of microbial networks in terrestrial environments.
222 Furthermore, increases in aridity have been shown to reduce soil microbial abundance (Maestre et al.
223 2015), to decouple nutrient cycles (Delgado-Baquerizo et al. 2013), and to raise abiotic stress in
224 drylands (Vicente-Serrano et al. 2012). Thus, soil properties, plant community attributes and microbial
225 abundance need to be considered when evaluating the role of increasing aridity as a driver of microbial
226 community assembly.

227 Before conducting SEMs, soil total organic C and total phosphorus were log-transformed to
228 improve linearity. Microbial abundance was introduced in the model as the average of the abundance of
229 bacteria and fungi (after \log_{10} -transformation and z-score standardization). We did so to allow the
230 inclusion of the fungal:bacterial ratio in our model, which otherwise would be highly correlated with
231 the abundance of total bacteria and fungi. Note that we included this ratio in our model to provide
232 further evidence that changes in the contribution from fungal and bacterial phylotypes to each module
233 considered the abundance of these organisms. Soil organic C was highly related to soil total N
234 (Spearman's $\rho = 0.820$; $p < 0.001$), and its inclusion represented soil organic matter in our models

235 (Delgado-Baquerizo et al. 2013). Because of this, total N was not explicitly included in the model. In
236 our SEM model, the different within-plot vegetation types (grasses, N-fixing shrubs and trees) were
237 categorical variables with two levels: 1 (particular microhabitat; e.g., trees) and 0 (remaining
238 microhabitats + open areas). Doing so allowed for comparison in the effect of a specific within-plot
239 vegetation type (e.g. trees) on each microbial module with the average of the remaining vegetation
240 types and open areas. Note that for our baseline condition (i.e. procedural control), we selected the
241 composite samples from open areas, and, therefore, did not explicitly include it in our model (Grace
242 2006). Using the same approach, we included in our model the most common soil types: Ustox
243 (Oxisols of semiarid and subhumid climates) and Albolls (Mollisols of wet soils), which were found in
244 95% of our studied sites.

245 We then tested model goodness of fit using the Chi-square (χ^2) test. A model has a good fit when
246 $0 \leq \chi^2 \leq 2$ and $0.05 < p \leq 1.00$) and the root mean square error of approximation (RMSEA; the model
247 has a good fit when $0 \leq RMSEA \leq 0.05$ and $0.10 < p \leq 1.00$). We then used the Bollen-Stine
248 bootstrap test (the model has a good fit when $0.10 < \text{bootstrap } p \leq 1.00$) to confirm model fit and our
249 results indicated that our *a priori* model had a good fit to our data.

250 Finally, we used Spearman correlations to identify particular microbial taxa within a given
251 module that are highly characteristic of particular aridity conditions (i.e., increase or decrease with
252 aridity). In particular, we correlated the relative abundance of all phylotypes within each major module
253 and aridity. These analyses were conducted using the R statistical software (<http://cran.r-project.org/>).
254 Spearman correlations were also used to explore the link between the relative abundance of a given
255 module and surrogates of multiple ecosystem functions including soil enzyme activities, available
256 nutrients and ANPP.

257

258 **Results**

259 We found that communities of fungi and bacteria grouped into four largely independent microbial
260 modules across our environmental gradient, accounting for 41.7, 57.7, 0.50 and 0.09% of the microbial
261 phylotypes, respectively (Fig. 1B). Each module represented a discrete, tightly correlated microbial
262 cluster, including phylotypes of both fungi and bacteria whose relative abundance was more strongly
263 associated with each other than with phylotypes from other clusters (Fig. 2). We retained in our
264 network analyses the first three modules, which accounted for 99.9% of microbial phylotypes. Module

265 #4 was not ubiquitous (i.e., it was present at only one site), and was therefore removed from further
266 statistical modeling. The relative abundances of Modules #1 and 2 were highly negatively correlated (ρ
267 = -0.999; $P < 0.001$). Modules 1 ($\rho = 0.276$; $p = 0.002$) and 2 ($\rho = 0.283$; $p = 0.002$) were also related to
268 Module #3. Modules #1 and #3 were dominated by fungal taxa, while Module #2 had a higher relative
269 contribution from bacteria (Figs. 2 and S1). Module #1 comprised 28% phylotypes of bacteria and 58%
270 phylotypes of fungi, and Module #2 comprised 61% phylotypes of bacteria and 31% phylotypes of
271 fungi (Fig. 2A).

272 Aridity was strongly negatively and positively related to the relative abundance of Module #1
273 (hereafter Mesic Module #1; defined as microbial taxa preferring more mesic environments) and #2
274 (hereafter Xeric Module #2; defined as microbial taxa preferring more arid environments), respectively,
275 accounting for 99.4% of all taxa in all locations across our environmental gradient (i.e. standardized by
276 microsite coverage; Figs. 2A and 2B). Module #3 was not significantly related to aridity (Figs. S2 and
277 S3). Similar results were found at the sample level (Fig. S3). These results were maintained when we
278 controlled for the spatial influence of the data (Figs. 2B). The relative abundances of Mesic Module #1
279 and Xeric Module #2 were strongly positively related to the relative abundances of the same modules
280 but calculated as the standardized sum of the relative abundance of each OTU within each module
281 (Spearman $\rho > 0.94$; $p < 0.001$). Moreover, similar results were found for the cross-validation network.
282 The SparCC Module #1 was significantly and positively related to Mesic Module #1 (Pearson's $r =$
283 0.47 ; $p < 0.001$), and SparCC Module #2 was significantly and positively related to Xeric Module #1
284 (Pearson's $r = 0.50$; $p < 0.001$). The SparCC analyses yielded an additional dominant module (SparCC
285 Module #3), which was also significantly and positively correlated to Mesic Module #1 (Pearson's $r =$
286 0.34 ; $p < 0.001$). More importantly, SparCC Module #1 was negatively related to aridity (Pearson's $r =$
287 0.27 ; $p = 0.003$), while SparCC Module #2 was positively related to aridity (Pearson's $r = 0.50$; $p =$
288 0.004).

289 Overall, our structural equation model explained 83% of the variation in both Mesic Module #1
290 and Xeric Module #2. Aridity had a direct negative effect on the relative abundance of Mesic Module
291 #1, while having a positive effect on the relative abundance of Xeric Module #2 (Figs. 3A). Moreover,
292 although the impacts of aridity on the relative abundance of the main modules were largely direct, we
293 also found that increases in aridity affected the assembly of the microbial correlation network indirectly
294 by shifting soil types from Albolls to Ustox, declining total plant cover and by increasing soil total P

295 and pH (Fig. 3A). We also found some direct and indirect effects of vegetation type on the relative
296 abundance of microbial modules (Fig. 3A). For example, the presence of trees had indirect negative and
297 positive effects on Mesic Module #1 and Xeric Module #2, respectively, via soil pH and P. The relative
298 abundance of Mesic Module #1 was positively correlated with multiple surrogates of ecosystem
299 functioning, including nutrient availability, enzyme activities and plant primary productivity (Table S1).

300 In general, we found that 2806 and 4676 microbial phylotypes within Mesic Module #1 and
301 Xeric Module #2 were negatively and positively correlated with aridity, respectively ($P < 0.05$; Table
302 S2). In particular, we found multiple microbial taxa from genus *Rubrobacter*, *Geodermatophilus* and
303 *Streptomyces* or class *Thermomicrobia* and phylotypes *Preussia minima*, *Alternaria triticimaculans*,
304 *Pleosporales* sp., *Fusarium tricinctum* and *Phoma macrostoma*, *Tulostoma melanocyclum*, *Geastrum*
305 *pectinatum*, *Laccaria* sp. and *Mortierella wolfii* to be strongly positively related to aridity (potential
306 winners; Fig. 4; Table S2). On the contrary, we found that microbial phylotypes including
307 *Cladophialophora* sp., *Trichoderma spirale*, *Oidiodendron* sp., *Helotiales* sp., *Pochonia bulbillosa*,
308 *Umbelopsis gibberispora* and *isabellina*, *Burkholderia tuberum*, *Sphingomonas wittichii*,
309 *Mycobacterium celatum* and *Actinomadura vinacea* were strongly negatively correlated with aridity
310 (potential losers; Fig. 4; Table S2). The complete list of taxa predicting aridity changes within each
311 module is available in Table S2.

312

313 Discussion

314 *Increases in aridity lead to dramatic changes in the assembly of soil microbial communities*

315 Our findings support the hypothesis that increases in aridity lead to significant changes in the relative
316 abundance of modules of tightly co-occurring fungal and bacterial phylotypes. In particular, our results
317 indicate that certain microbial modules will be susceptible to increases in aridity, particularly in the
318 transition between semi-arid and arid areas (where Mesic Module #1 shifted to Xeric Module #2).
319 Previous studies have shown that increases in aridity negatively affect microbial diversity and
320 abundance (Maestre et al. 2015). Here, we provide solid evidence that increases in aridity, just as those
321 predicted under climate change, can promote marked changes in the assembly of complex microbial
322 networks at the regional scale, leading to substantial turnover of entire microbial communities. These
323 changes may result in local extinctions in terrestrial ecosystems. Moreover, we were able to identify
324 particular taxa of fungi and bacteria at the OTU level (phylotype level) that are strongly negatively

325 (losers) or positively (winners) related to increases in aridity in eastern Australia. These results provide
326 a regional list of particular microbial phylotypes that could be highly vulnerable to predicted increases
327 in aridity in this century. These results have implications for our understanding of processes related to
328 land degradation and desertification, such as overgrazing and land clearance, which are likely to
329 become more pronounced as we move to a drier and more unpredictable climate.

330 An important result from our study was that increases in aridity shifted the network of
331 associations from a dominance by fungal phylotypes (in terms of OTU relative abundance and number
332 of phylotypes) associated with bacteria (Mesic Module #1) to bacterial phylotypes co-occurring with
333 fungi (Xeric Module #2). In support of these results, our SEM showed that the fungal:bacterial ratio
334 declined with increasing aridity. Soil bacteria and fungi include mutualistic, neutral, pathogenic and
335 parasitic relationships, and their complex associations are linked to essential ecosystem processes such
336 as litter decomposition (Kobayashi and Crouch 2009). Changes in the relative contribution of
337 phylotypes of bacteria and fungi to the network of microbial associations might then alter soil
338 functioning in terrestrial ecosystems. Bacteria and fungi are known to be involved in different processes
339 that are fundamental for sustaining a functional ecosystem (van der Heijden et al. 2008). For example,
340 bacterial-dominated microbial communities often lead to fast cycling of nutrient (e.g. nitrification) and
341 to open nutrient cycling (i.e., lower capacity to retain nutrients in the system; van der Heijden et al.
342 2008). Moreover, slow-growing organisms such as soil fungi have been reported to promote the
343 resistance of nutrient cycling to climate change compared with fast-growing organisms such as bacteria
344 (van der Heijden et al. 2008). Thus, by promoting changes in the contribution of bacteria over fungi
345 phylotypes to the network of associations, increases in aridity might indirectly impact the provision and
346 resistance of essential ecosystem functions and services such as litter decomposition and nutrient
347 cycling (Kobayashi and Crouch 2009).

348 *Direct and indirect effects of aridity on the relative abundance of microbial modules.*

349 We found that aridity regulated the relative abundance of main microbial modules both directly, i.e. via
350 reductions in water availability, and indirectly, via changes in soil type, soil properties such as soil P
351 and pH, and total plant cover, which are known to be impacted by aridity (Delgado-Baquerizo et al.
352 2013; Maestre et al. 2015). Part of these effects might be associated with the fact that soils in Australian
353 drylands are old, acidic and nutrient-depleted, compared with other drylands (Eldridge et al. 2018b).
354 For example, increases in soil pH associated with increasing aridity may explain the observed changes

355 in the assembly of these networks. Soil pH has been widely reported to be an important driver of
356 microbial communities in terrestrial ecosystems. However, this is not always the case for drylands
357 where pH is typically high, and microbial communities are less sensitive to changes in pH (Maestre et
358 al. 2015; Neilson et al. 2017). Similarly, increases in soil P with aridity may play a major role in
359 driving the soil microbial networks studied, as Australian environments are known to be strongly P-
360 limited, with reported consequences for the biodiversity and functioning of biotic communities
361 (Lambers et al. 2013). Reductions in plant cover associated with increases in aridity might also alter the
362 complete microbial network of associations via reductions in resource inputs (e.g. litter and
363 rhizodeposition) and exacerbating specific harsh environmental conditions (e.g. amount of radiation).
364 Our findings indicate that soil variables such as pH and total P –linked to changes in soil type with
365 increases in aridity–, and plant cover, which are important predictors of microbial community
366 composition and diversity (Tedersoo et al. 2014; Maestre et al. 2015), are also key drivers of the
367 complex network of bacterial and fungal phylotypes associations in soils. Some of these findings have
368 strong implications for forecasting climate change impacts on microbial networks. For example, trees
369 had indirect negative and positive effects, respectively, on Mesic Module #1 and Xeric Module #2 via
370 soil pH and soil P. Interestingly, plant cover and richness had multiple direct effects on the relative
371 abundance of Mesic Module #1 and Xeric Module #2. These results highlight the importance of
372 microsite differentiation in controlling the assembly of complex microbial networks via changes in
373 local soil properties. Moreover, this result further suggests that changes in vegetation functional
374 composition in response to increasing aridity will have indirect consequences for the relative abundance
375 of key microbial modules in terrestrial environments. For example, increases in aridity are linked to
376 reduced cover of trees (Table S3). Further, the cover of trees was positively/negatively linked to the
377 relative abundance of Mesic Module #1 and Xeric Module #2, respectively (Table S3). Thus, changes
378 in the relative abundance of this within-plot vegetation type could impact the assembly of microbial
379 networks in terrestrial ecosystems, with potential collateral effects for ecosystem functioning. These
380 results are in accordance with a recent study evaluating changes in microbial diversity along a regional
381 aridity gradient in Chile (Neilson et al. 2017).

382 Our SEM model supports the hypothesis that increasing aridity will lead to the turnover of
383 entire microbial communities in terrestrial ecosystems by shifting the relative abundance of well-
384 defined microbial modules (from Mesic Module #1 to Xeric Module #2). Given the observed links

385 between network structure and ecosystem functioning, we expect these shifts to have strong
386 implications for ecosystem functioning under a changing climate. For example, we found that the
387 relative abundance of Mesic Module #1 was positively related to variables such as the activity of
388 phosphatase, the amount of available soil C and inorganic N and ANPP, which are all linked to
389 ecosystem functions and services such as nutrient cycling, organic matter decomposition and
390 mineralization and food production (Table S1). Thus, our results propose the idea that changes in the
391 complex network of microbial associations derived from increased aridity might negatively impact
392 ecosystem processes linked to the provision of key ecosystem services. Moreover, these findings
393 further support the results of a previous metagenomics study reporting large differences in potential soil
394 functioning between arid and humid environments (Fierer et al. 2012). Future endeavors exploring
395 modules of microbial communities co-occurring in terrestrial ecosystems should further evaluate the
396 functional attributes of microbial modules so that we can gain further functional insights on the role of
397 microbial networks in regulating ecosystem functioning.

398 *Winners and losers microbial taxa in response to increasing aridity.*

399 We identified microbial taxa that are potentially vulnerable (losers) or might benefit (winners) from
400 predicted increases in aridity throughout this century (Huang et al. 2016; Neilson et al. 2017). Microbial
401 losers are expected to be phylotypes unable to tolerate the increasingly harsh conditions associated with
402 aridity, including water scarcity or extreme radiation derived from reductions in plant coverage. Here,
403 we found that increases in aridity may reduce the relative abundance of some microbial phylotypes
404 within Mesic Module #1, which are linked to the performance of plants via symbiosis such as
405 *Burkholderia tuberum* (capable of symbiotic nitrogen fixation with some legumes; Esqueda et al. 2012)
406 and *Oidiodendron* sp. (ericoid mycorrhiza; Smith and Read 2008). In addition, we found that important
407 taxa such as *Helotiales* sp. (saprobes) and *Sphingomonas wittichii* (involved in toxin degradation)
408 might be negatively influenced by increases in aridity, with consequences for overall ecosystem
409 functioning. Interestingly, the parasitic nematode *Pochonia bulbillosa* was also found to decline with
410 increases in aridity, suggesting that, as found with soil animals and vascular plants (Vicente-Serrano et
411 al. 2012), associated microbial phylotypes will also be negatively impacted by increases in aridity.

412 We also found multiple phylotypes whose relative abundance increased with aridity. Winners,
413 i.e. phylotypes which can potentially benefit from increases in aridity along this century, are expected
414 to be thermophilic and highly resistant to desiccation and radiation. Interestingly, taxa from Xeric

415 Module #2 included a wide variety of taxa typical from desert ecosystems, which are noted radiation
416 and desiccation tolerant desert bacteria including phylotypes from the genus *Rubrobacter*,
417 *Geodermatophilus*, *Streptomyces* or from the class *Thermomicrobia* (Mohammadipanah and Wink
418 2016). All these taxa were strongly positively correlated with aridity. We also found fungal phylotypes
419 typical from drylands, such as *Tulostoma melanocyclus*, *Preussia minima* and *Geastrum pectinatum*, to
420 be strongly positively related to aridity (Esqueda et al. 2004). We also found that increasing aridity had
421 a strong positive correlation with the relative abundance of multiple fungal pathogens of plants,
422 including *Alternaria triticimaculans*, *Pleosporales sp.*, *Pleosporaceae sp.*, *Fusarium tricinctum* and
423 *Phoma macrostoma*. We also found that the relative abundance of *Mortierella wolfii*, a well-known
424 pathogen of humans and other animals that can cause bovine abortion and pneumonia (Davies and
425 Wobeser 2010), increased with aridity. Other fungal taxa such as *Capronia peltigerae* –a parasite of
426 living lichens– also increased in the most arid places, where biocrust-forming lichens are often
427 abundant (Liu et al. 2017). Building on from previous efforts aiming to identify the role of aridity in
428 regulating microbial communities in drylands (Maestre et al. 2015; Neilson et al. 2017), our study
429 improves our understanding and provides evidence for potential winner and loser taxa in response to
430 increases in aridity in Australia.

431 *Conclusions*

432 All things considered, our findings present strong evidence that increases in aridity will lead to critical
433 shifts in the assembly of complex microbial networks of fungi and bacteria, potentially leading to
434 massive phylotype exchange and local extinctions in terrestrial ecosystems, as demonstrated by the
435 reductions of up to 97% in the relative abundance of microbial taxa within Mesic Module #1. Our
436 results thus fill major gaps in our understanding of how complex networks of microbial associations
437 respond to increases in aridity, which will promote land degradation in drylands worldwide, and
438 provide solid evidence of the vulnerability of microbial networks to climate change. Considering the
439 primacy of microbial communities in ecosystem functioning, the reported changes in the assembly of
440 microbial co-occurrence networks are likely to have far-reaching consequences for the provision of
441 important ecosystem functions and services like litter break-down, nutrient cycling and plant
442 productivity, and hence need to be considered when assessing the consequences of climate change and
443 associated land degradation on the functioning of terrestrial ecosystems.

444

445 **Acknowledgments**

446 This research is supported by the Australian Research Council projects DP190103714 and
447 DP170104634. We thank Melissa S. Martin for revising the English of this manuscript. DBS
448 acknowledges the support of a Marsden Fast-Start Grant and a Rutherford Discovery Fellowship, both
449 administered by the Royal Society of New Zealand. M.D-B. acknowledges support from the Marie
450 Sklodowska-Curie Actions of the Horizon 2020 Framework Programme H2020-MSCA-IF-2016 under
451 REA grant agreement n°702057. DJE was supported by the Hermon Slade Foundation. FTM
452 acknowledges support from the European Research Council (BIODESERT project, ERC Grant
453 agreement n°647038), the Spanish Ministerio de Economía y Competitividad (BIOMOD project, ref.
454 CGL2013-44661-R) and from a Humboldt Research Award from the Alexander von Humboldt
455 Foundation.

456 **Data accessibility**

457 The primary data have been deposited in figshare: <https://figshare.com/s/5c12e197707e753dbfaa> (DOI:
458 10.6084/m9.figshare.7571399). The raw sequence data have been deposited in figshare:
459 <https://figshare.com/s/55813554972fd4a51195> (DOI: 10.6084/m9.figshare.7092950).

461 **References:**

- 462 Barberán, A., Bates, S.T., Casamayor, E.O., Fierer, N. (2012) Using network analysis to explore co-
463 occurrence patterns in soil microbial communities. *ISME J.* 6, 343-351.
- 464 Bell, C.W., Fricks, B.E., Rocca, J.D., Steinweg, J.M., McMahon, S.K., Wallenstein, M.D. (2013)
465 High-throughput Fluorometric Measurement of Potential Soil Extracellular Enzyme Activities. *J Vis*
466 *Exp* e50961, doi,10.3791/50961.
- 467 Blondel, V. D., Guillaume J.-L., Lambiotte R., and Lefebvre E., (2008) Fast unfolding of
468 communities in large networks. *J. Stat. Mech.* P10008
- 469 Caporaso, J.G., Kuczynski, J., Stombaugh, J., Bittinger, K., Bushman, F.D., Costello, E.K. Fierer N,
470 Peña AG, Goodrich JK, Gordon JJ, Huttley GA, Kelley ST, Knights D, Koenig JE, Ley RE,
471 Lozupone CA, McDonald D, Muegge BD, Pirrung M, Reeder J, Sevinsky JR, Turnbaugh PJ,
472 Walters WA, Widmann J, Yatsunenko T, Zaneveld J, Knight R. (2010). QIIME allows analysis of
473 high-throughput community sequencing data. *Nature Methods* 7, 335-336.

474 Davies J.L. Wobeser, G.A. (2010) Systemic infection with *Mortierella wolfii* following abortion in
475 a cow. *Can Vet J.* 51, 1391–3.

476 Delgado-Baquerizo, Maestre FT, Gallardo A, Bowker MA, Wallenstein MD, Quero JL, Ochoa V,
477 Gozalo B, García-Gómez M, Soliveres S, García-Palacios P, Berdugo M, Valencia E, Escolar C,
478 Arredondo T, Barraza-Zepeda C, Bran D, Carreira JA, Chaieb M, Conceição AA, Derak M,
479 Eldridge DJ, Escudero A, Espinosa CI, Gaitán J, Gatica MG, Gómez-González S, Guzman E,
480 Gutiérrez JR, Florentino A, Hepper E, Hernández RM, Huber-Sannwald E, Jankju M, Liu J, Mau
481 RL, Miriti M, Monerris J, Naseri K, Noumi Z, Polo V, Prina A, Pucheta E, Ramírez E, Ramírez-
482 Collantes DA, Romão R, Tighe M, Torres D, Torres-Díaz C, Ungar ED, Val J, Wamiti W, Wang D,
483 Zaady E. (2013). Decoupling of soil nutrient cycles as a function of aridity in global drylands.
484 *Nature* 502, 672–676.

485 Delgado-Baquerizo M., F.T. Maestre, P.B. Reich, P. Trivedi, Y. Osanai, Y. Liu, K. Hamonts, T.C.
486 Jeffries, B.K. Singh (2016). Carbon content and climate variability drive global soil bacterial
487 diversity patterns. *Ecol. Monogr.* 3, 373–390.

488 Delgado-Baquerizo M, Eldridge DJ, Ochoa V, Gozalo B, Singh BK, Maestre FT. (2017) Soil
489 microbial communities drive the resistance of ecosystem multifunctionality to global change in
490 drylands across the globe. *Ecology Letters* 20,1295-1305.

491 Delgado-Baquerizo M, Oliverio AM, Brewer TE, Benavent-González A, Eldridge DJ, Bardgett RD,
492 Maestre FT, Singh BK, Fierer N. (2018a). A global atlas of the dominant bacteria found in soil.
493 *Science* 359 (6373), 320-325.

494 DeSantis, T.Z., Hugenholtz P, Larsen N, Rojas M, Brodie EL, Keller K, Huber T, Dalevi D, Hu P,
495 Andersen GL. (2006). Greengenes, a chimera-checked 16S rRNA gene database and workbench
496 compatible with ARB. *Appl. Environ. Microbiol.* 72, 5069-72.

497 Edgar, R.C. (2010). Search and clustering orders of magnitude faster than BLAST. *Bioinformatics*
498 26, 2460.

499 Eldridge, D. J., Delgado-Baquerizo, M., Travers, S. K., Val, J., & Oliver, I. (2018a). Livestock
500 grazing and forest structure regulate the assembly of ecological clusters within plant networks in
501 eastern Australia. *Journal of Vegetation Science*, 29, 788-797.

502 Eldridge, D. J., Maestre, F. T. Koen B., Delgado-Baquerizo M. (2018b). Australian dryland soils
503 are acidic and nutrient-depleted, and have unique microbial communities compared with other
504 drylands. *Journal of Biogeography* 45, 2803-2814.

505 Fierer, N., Leff JW, Adams BJ, Nielsen UN, Bates ST, Lauber CL, Owens S, Gilbert JA, Wall DH,
506 Caporaso JG. (2012). Cross-biome metagenomic analyses of soil microbial communities and their
507 functional attributes. *Proc. Natl. Acad. Sci. USA.* 109, 21390-21395.

508 Friedman, J. & Alm, E.J. (2017). Inferring correlation networks from genomic survey data. *PLoS*
509 *Comput. Biol.* 8, e1002687.

510 Grace, J.B. (2006). *Structural Equation Modeling Natural Systems* (Cambridge Univ. Press,
511 Cambridge).

512 Huang, J., Yu, H., Guan, X., Wang, G., Guo, R. (2016). Accelerated dryland expansion under
513 climate change. *Nat. Clim. Change* 6, 166–171.

514 Liu, Y-R., Delgado-Baquerizo, M., Trivedi, P., He, Y-Z., Wang, J-T., Singh, B.K. (2017). Identity of
515 biocrust species and microbial communities drive the response of soil multifunctionality to
516 simulated global change. *Soil Biol Biochem* 107, 208-217.

517 Maestre, F.T., Delgado-Baquerizo M, Jeffries TC, Eldridge DJ, Ochoa V, Gozalo B, Quero JL,
518 García-Gómez M, Gallardo A, Ulrich W, Bowker MA, Arredondo T, Barraza-Zepeda C, Bran D,
519 Florentino A, Gaitán J, Gutiérrez JR, Huber-Sannwald E, Jankju M, Mau RL, Miriti M, Naseri K,
520 Ospina A, Stavi I, Wang D, Woods NN, Yuan X, Zaady E, Singh BK. Increasing aridity reduces soil
521 microbial diversity and abundance in global drylands. *Proc. Natl. Acad. Sci. USA* 112, 15684–
522 15689.

523 Mohammadipanah, F. and Wink, J. (2016) Actinobacteria from Arid and Desert Habitats: Diversity
524 and Biological Activity. *Front. Microbiol.* 6, 1541.

525 Neilson, J.W., Califf, K., Cardona, C., Copeland, A., van Treuren, W., Josephson, K.L., Knight, R.,
526 Gilbert, J.A., Quade, J., Caporaso, J.G., Maier, R.M. (2017). Significant impacts of increasing
527 aridity on the arid soil microbiome. *mSystems* 30: e00195-16.

528 Newman, M.E.J., Girvan M. (2004). Finding and evaluating community structure in networks.
529 *Phys. Rev.* 69, 26113.

530 Shi, S., Nuccio, E.E., Shi, Z.J., He, Z. Zhou, J., Firestone, M.K. (2016). The interconnected
531 rhizosphere: High network complexity dominates rhizosphere assemblages. *Ecol Lett* 6, 926-36.

532 Smith, S. E., Read, D. J. (2008). *Mycorrhizal Symbiosis*, Third Edition. Academic Press.
533 Stouffer, D.B., Bascompte, J. (2011). Compartmentalization increases food-web persistence. *Proc.*
534 *Natl. Acad. Sci. USA* 108, 3648–3652.
535 Tedersoo, L., Bahram M, Põlme S, Kõljalg U, Yorou NS, Wijesundera R, Villarreal Ruiz L, Vasco-
536 Palacios AM, Thu PQ, Suija A, Smith ME, Sharp C, Saluveer E, Saitta A, Rosas M, Riit T,
537 Ratkowsky D, Pritsch K, Põldmaa K, Piepenbring M, Phosri C, Peterson M, Parts K, Pärtel K,
538 Otsing E, Nouhra E, Njouonkou AL, Nilsson RH, Morgado LN, Mayor J, May TW, Majuakim L,
539 Lodge DJ, Lee SS, Larsson KH, Kohout P, Hosaka K, Hiiesalu I, Henkel TW, Harend H, Guo LD,
540 Greslebin A, Grelet G, Geml J, Gates G, Dunstan W, Dunk C, Drenkhan R, Dearnaley J, De Kesel
541 A, Dang T, Chen X, Buegger F, Brearley FQ, Bonito G, Anslan S, Abell S, Abarenkov K. (2014).
542 Fungal biogeography Global diversity and geography of soil fungi. *Science* 28, 346.
543 van der Heijden, M.G., Bardgett, R.D., van Straalen, N.M. (2008). The unseen majority, soil
544 microbes as drivers of plant diversity and productivity in terrestrial ecosystems. *Ecol. Lett.* 11, 296-
545 310.
546 van Dongen, S.M. (2000). *Graph Clustering by Flow Simulation*. Ph.D. thesis, Universtiy of
547 Utrecht.
548 Vincent, P, Larochelle, H, Bengio, Y, Manzagol, P-A. Extracting and composing robust features
549 with denoising autoencoders (2008). In *Proceedings of the 25th International Conference on*
550 *Machine learning*, pp. 1096–1103. ACM. URL <http://dl.acm.org/citation.cfm?id=1390294>.
551 Vicente-Serrano, S.M., Gouveia C, Camarero JJ, Beguería S, Trigo R, López-Moreno JJ, Azorín-
552 Molina C, Pasho E, Lorenzo-Lacruz J, Revuelto J, Morán-Tejeda E, Sanchez-Lorenzo A. (2012).
553 Response of vegetation to drought time-scales across global land biomes. *Proc. Natl. Acad. Sci.*
554 *USA* 110, 52-57.

555 **Author contributions**

556 M.D-B. designed this study in consultation with D.B.S. Field data were collected by M.D-B. and D.J.E.
557 Soil analyses were conducted by F.T.M. Sequencing data was provided by B.K.S. Bioinformatic
558 analyses were done by T.C.J. Network analyses were done by D.B.S., G.D. and J.W in consultation
559 with J.R.P. The manuscript was written by M.D-B, edited by D.J.E., B.K.S., D.B.S. and F.T.M., and all
560 authors contributed substantially to the revisions.

561

562

563

564

565

566

567

568

569

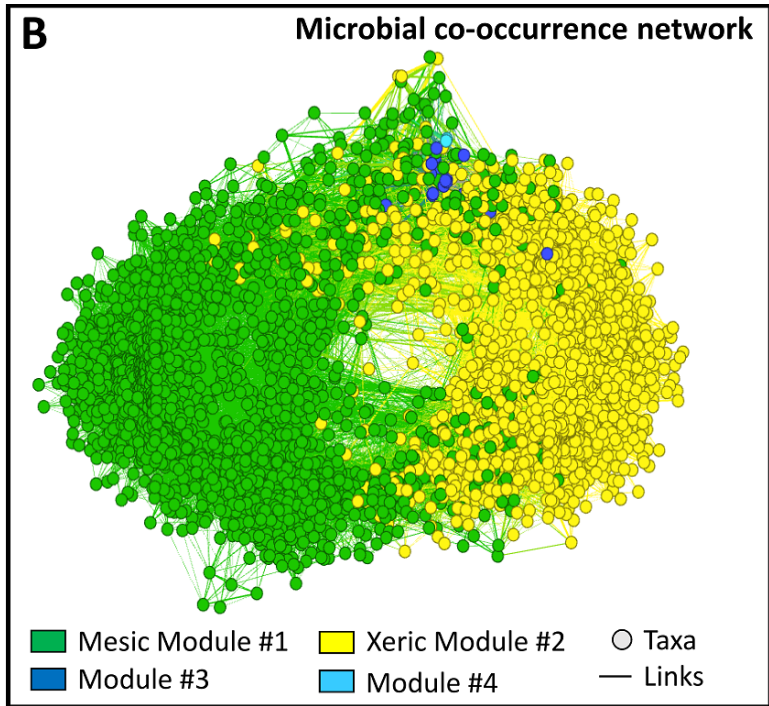
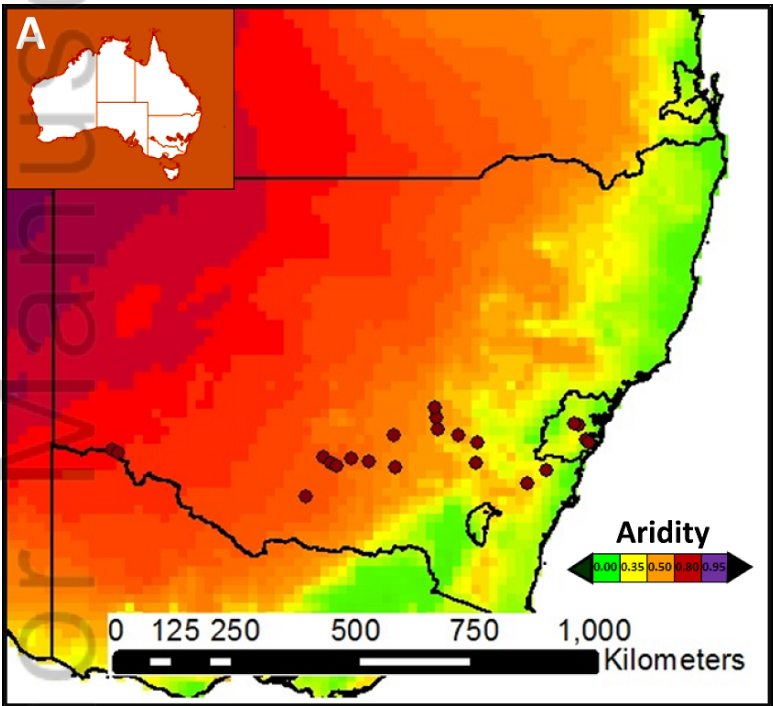
570 **Figure caption**

571 **Figure 1.** Location of the study sites studied (a), and correlation network including multiple nodes
572 (taxa) from bacteria and fungi (b). Color patterns in panel (a) indicate aridity (1 – aridity index)
573 gradients. Different colors in panel (b) correspond with different modules.

574 **Figure 2.** Community composition and association with increases in aridity for Mesic Module #1 and
575 Xeric Module #2. Panel (A) shows the overall bacterial and fungal community composition for Mesic
576 Module #1 and Xeric Module #2. Panel (B) shows the relationships between aridity and the relative
577 abundance of microbial modules at the site level. Results of regressions are as follows: Mod#1.
578 Ordinary least squares (OLS) (continuous line), $R^2 = 0.566$, $P < 0.001$, $AICc = 6.184$; Spatial
579 autoregressive analyses (SAR), $R^2 = 0.451$, $P = 0.001$, $AICc = 10.847$; Mod#2. OLS (continuous line),
580 $R^2 = 0.565$, $P < 0.001$, $AICc = 6.251$; SAR, $R^2 = 0.453$, $P = 0.001$, $AICc = 10.819$. Separate regressions
581 at the sample level are shown in Fig. S3.

582 **Figure 3.** Structural equation model fitted to the relative abundance of microbial Modules #1 and #2 (a)
583 and standardized total effects (direct plus indirect effects) derived from them (b). Numbers adjacent to
584 arrows are path coefficients (P values), and are indicative of the effect size of the relationship. R^2 = the
585 proportion of variance explained. P = Soil total P; C = Soil total organic C; F:B ratio = fungal: bacterial
586 ratio. Vegetation = within-plot vegetation type (trees, shrubs and grasses). Mods #1 and #2 = Mesic
587 Module #1 and Xeric Module #2, respectively. P -values as follow: * $P < 0.05$; ** $P < 0.01$.

588 **Figure 4.** Relationships between aridity and the relative abundance of selected phylotypes within Mesic
589 Module #1 and Xeric Module #2. A more completed list of examples for phylotypes within Mesic
590 Module #1 and Xeric Module #2 and their correlation (Spearman) to aridity is available in Table S2.

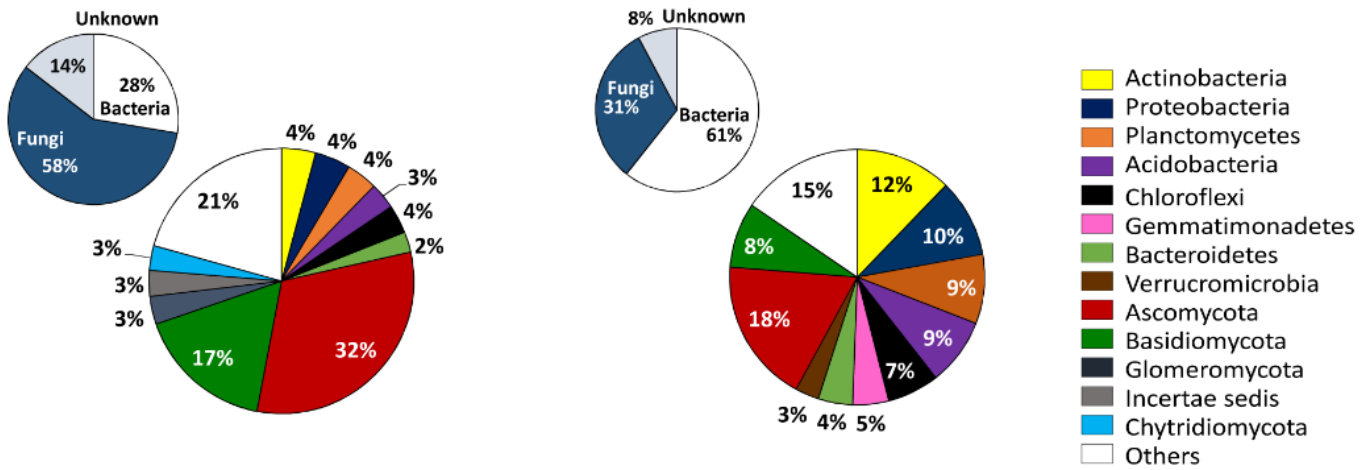


LDR_3453_f1.tif

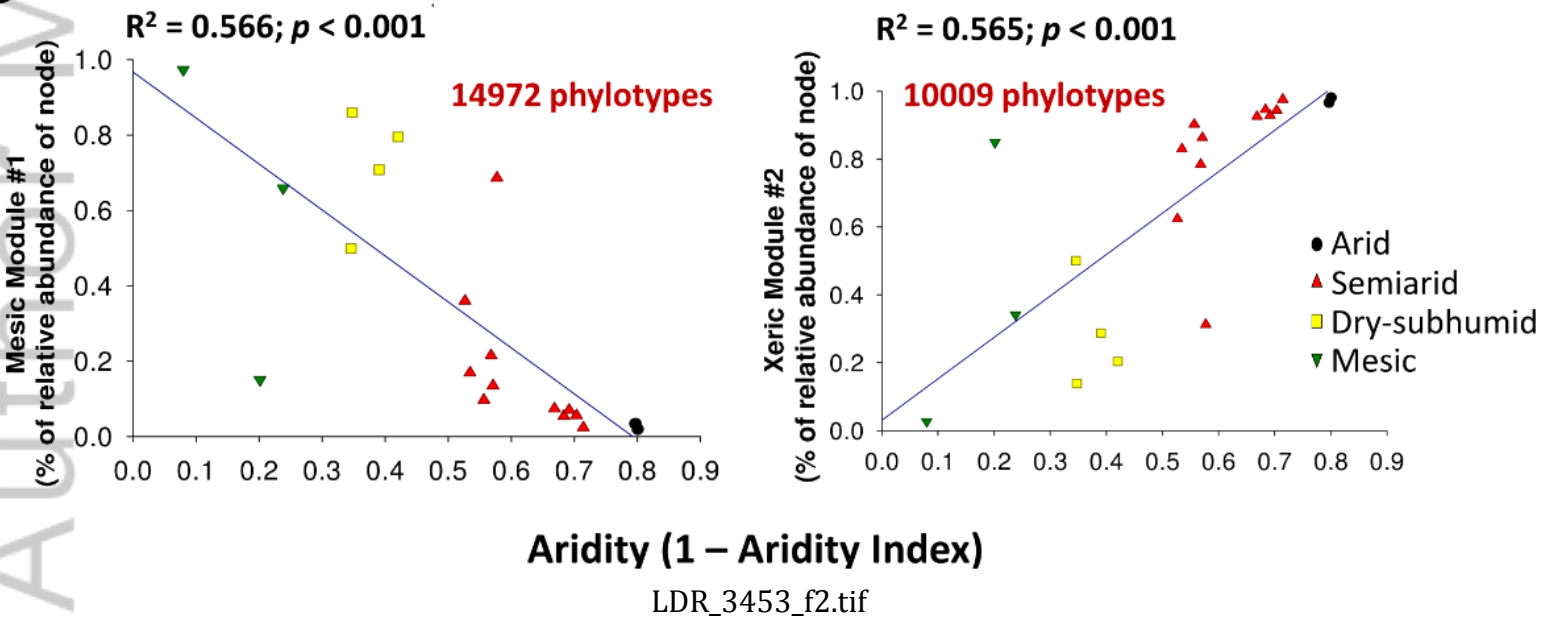
A

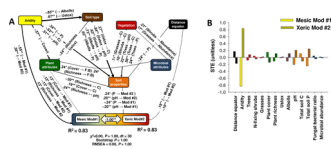
Mesic Module #1

Xeric Module #2

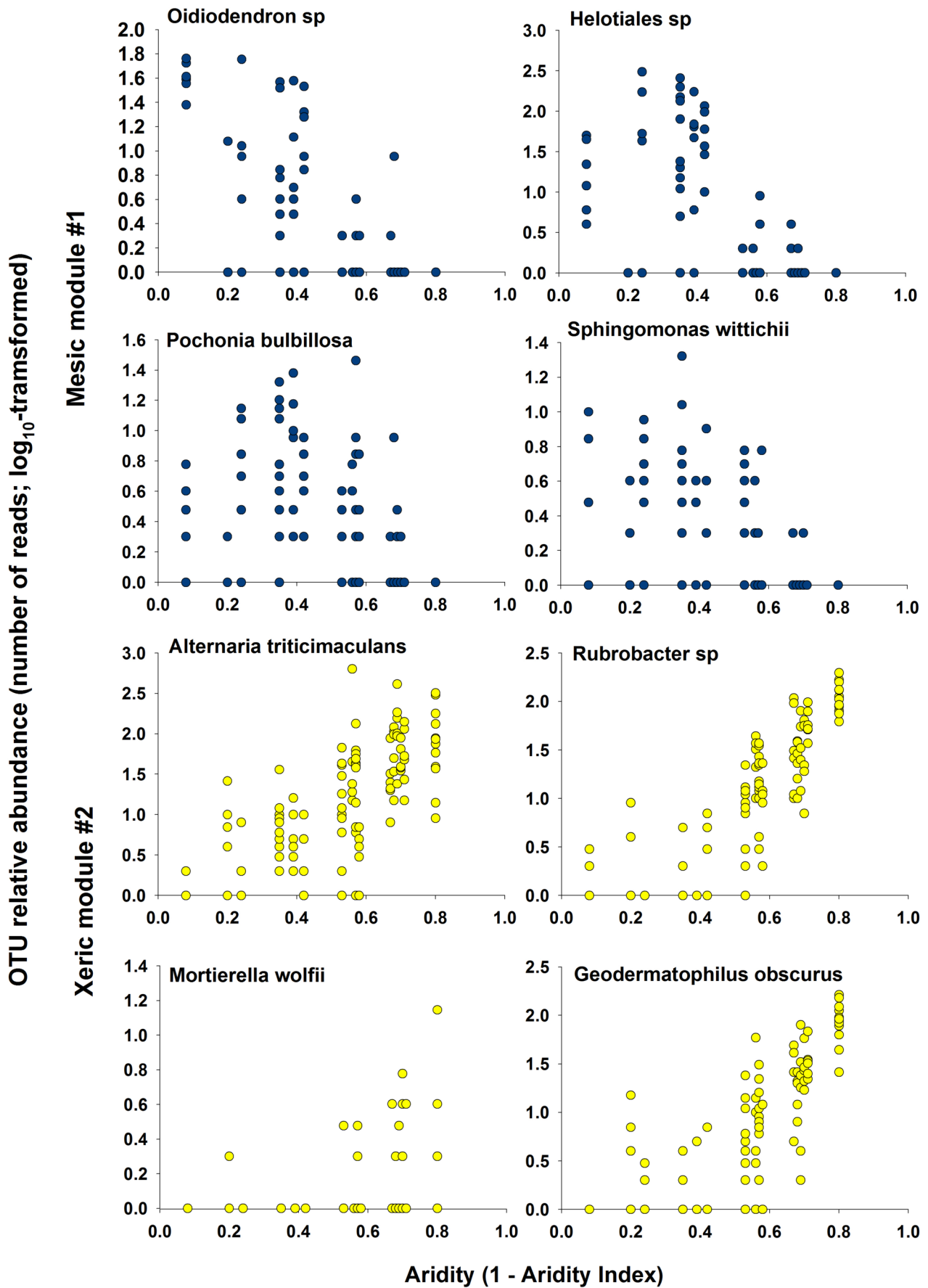


B





LDR_3453_f3.tif



LDR_3453_f4.tif